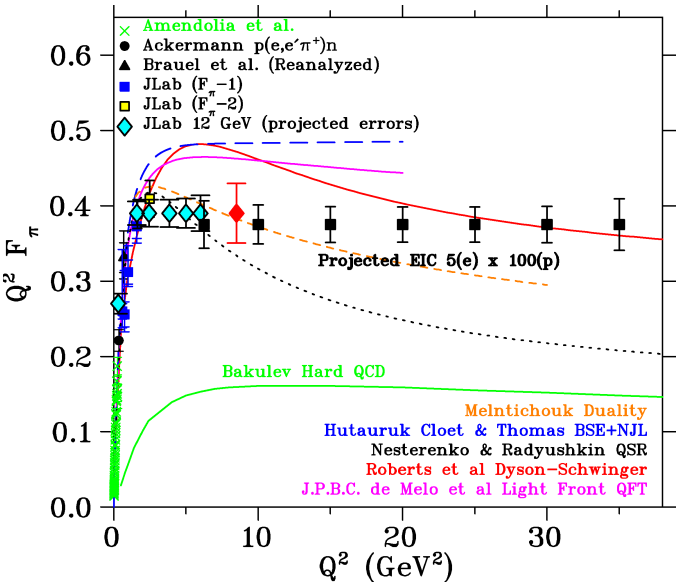

Figure 7.37: Existing data (blue, black, yellow, green) and projected uncertainties for future data on the pion form factor from JLab (cyan, red) and EIC (black), in comparison to a variety of hadronic structure models. The EIC projections clearly cover a much larger Q^2 range than the JLab measurements.

K^+ Form Factor The reliability of the electroproduction method to determine the K^+ form factor is not yet established. JLab E12-09-011 has acquired data for the $p(e,e'K^+)\Lambda$, $p(e,e'K^+)\Sigma^0$ reactions at hadronic invariant mass $W = \sqrt{(p_K + p_{\Lambda,\Sigma})^2} > 2.5$ GeV, to search for evidence of scattering from the proton's "kaon cloud". The data are still being analyzed, with L/T-separated cross sections expected in the next ∼2 years. If they confirm that the scattering from the virtual K^+ in the nucleon dominates at low four-momentum transfer to the target $|t| \ll m_p^2$, the experiment will yield the world's first quality data for F_K above $Q^2 > 0.2$ GeV^2. This would then open up the possibility of using exclusive reactions to determine the K^+ form factor over a wide range of Q^2 at higher energies. Studies are planned. While the general technique will remain the same, the π^-/π^+ validation technique to confirm the σ_L extraction cannot be used for the K^+. We are optimistic that Λ/Σ^0 ratios can play a similar role, however, conditions under which the clean separation of these two channels may be possible at the EIC requires further study and would only be possible at CM energies of ∼10-50 GeV.

7.2.2 Imaging of quarks and gluons in position space

A key challenge of nuclear physics is the tomographic imaging of the nucleon, encoded in the Generalized Parton Distribution functions (GPDs). They provide a connection between ordinary parton distribution functions and form factors and hence can describe the correlations between the longitudinal momentum of quarks and gluons and their position in the transverse spatial plane in a nucleon [52, 211].

GPDs depend on three variables (considering the dependence on the factorization scale Q^2 to be known): x, that is the average longitudinal momentum of the active quark as a fraction of the average target momentum; ξ and t, that are, respectively, half the change in the fraction of longitudinal momentum carried by the struck parton and the squared four-momentum transferred to the hadron target. However, one does not have direct experimental access to this multidimensional structure, since the dependence on the three variables enters observables in nontrivial convolutions with coefficient functions. Since no single process is sufficient to determine GPDs fully, measurement of a variety of processes and observables is necessary to maximally constrain them. Fits of GPDs require educated assumptions for the choice of the fitting functions to incorporate the known theoretical constraints of GPDs, i.e. polinomiality, sum rules, and positivity (see, e.g., Refs. [52, 211–215] for a detailed preface to the GPD formalism and properties). Owing to the factorization property of QCD, a number of related processes are complementary to disentangle the various GPDs and their flavor dependence (see, e.g., Refs. [216–218] for recent works on the GPD phenomenology).

Phenomenology of GPDs

The cleanest way to access GPDs is via exclusive electroproduction of a real photon - a process known as deeply virtual Compton scattering (DVCS) - off a nucleon target at high photon virtuality and low momentum transfer, where the scattering happens from a single parton [219] (see diagram (a) in Fig. 7.38).

Because of a relative simplicity of this process, it is well described theoretically, including higher orders in α_s, higher-twist and target mass corrections (for a comprehensive review see e.g Ref. [216]).

The DVCS cross-section is parametrized in terms of Compton form factors (CFFs), through which the full range of x is not directly accessible. CFFs are complex functions whose real part yields the integral of a GPD over x, while the imaginary part is the GPD at the $x = \pm\xi$ line. Experimentally, cross-sections, double-spin asymmetries and the beam-charge

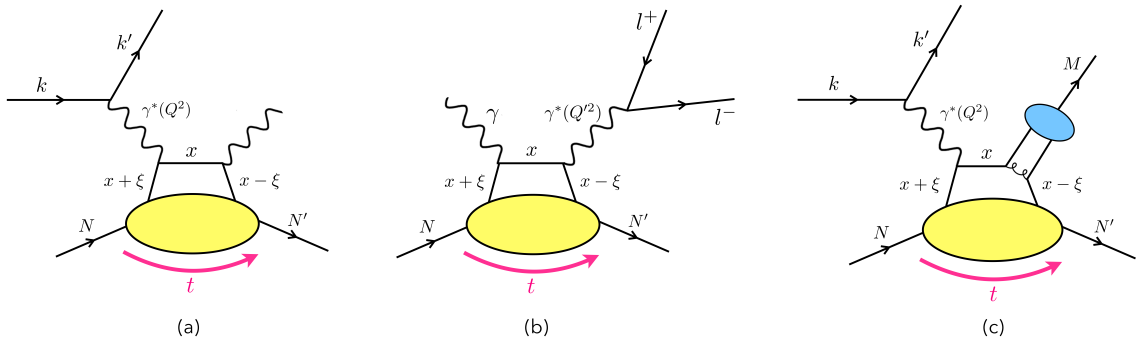

Figure 7.38: Illustrations of three main processes which carry sensitivity to GPDs: a) DVCS, b) TCS and c) one of the possible DVMP diagrams.

asymmetry (from measurements with both electron and positron beams) are sensitive to the real part of CFFs, while single spin asymmetries are parametrized in terms of their imaginary parts.

Timelike Compton scattering (TCS) is a related process in which a real photon scatters off a parton to produce a virtual photon, detected through its lepton-pair decay (see diagram (b) in Fig. 7.38) [220–224]. As such, this is an inverse process to DVCS, sensitive to the same set of GPDs. The complementarity of DVCS and TCS processes [223] relies mostly on consequences of the analyticity of the Q^2 behaviour of amplitudes, as discussed in [224]. Confronting DVCS and TCS results together is a mandatory goal of the EIC to prove the consistency of the collinear QCD factorization framework and test the universality of GPDs. The differences in the two processes additionally give experimental advantages in the extraction of CFFs – for example the asymmetries associated with the lepton decay in TCS provide a more direct access to the real part of the dominant CFF [113].

Additional information on GPDs can be obtained from hard exclusive meson electroproduction, where a meson, instead of the photon, is produced as a result of the scattering (see diagram (c) in Fig. 7.38) [217]. These processes include:

> [(a)]heavy meson (J/ψ, Υ) electroproduction, which probes gluon-GPDs and may provide important new information on the underlying mechanism of saturation observing the change of the spatial gluon distribution from high to low Bjorken-x [225]; light vector meson (ρ^0; ρ^+; ω; ϕ) electroproduction, which in addition allows one to separate quark flavor GPDs; light pseudoscalar meson (π^+; π^0; η) electroproduction, which gives access to a group of chiral-odd GPDs that are inaccessible in DVCS at leading twist. Some of these GPDs are related to the transversity distributions extensively studied in SIDIS and Drell-Yan processes.

Hard exclusive production of π^0 mesons have final state similar to that of DVCS. It consists of one scattered lepton in DIS regime ($Q^2 > 1$ GeV^2), one scattered nucleon in a coherent state (i.e., no break of target particle in the interaction), and either one or two photons, for DVCS and DVMP π^0-decay, respectively. This similarity suggests that a common analysis of the detector requirements for both processes can be performed, as discussed in Sec. 8.4.1.

The information that can be extracted from a handful of DVCS measurements at low x_B by HERA collider experiments, almost entirely consisting of cross sections in loose $Q^2 - t$ bins, is very limited. GPD-based experiments at larger values of x_B have been carried out at HERMES and COMPASS. Dedicated fixed target experiments at the upgraded CEBAF 12 GeV facility at JLab are addressing GPDs in the kinematical region dominated by valence-quarks. More precise data mapping with high granularity and a wider phase space, are required to fully constrain the entire set of GPDs for gluons and sea quarks.

The EIC will cover a much larger phase-space, connecting the domain typical of fixed target experiments with that of collider measurements. With its wide range in energy and high luminosity, EIC will thus offer an unprecedented opportunity for a precise determination of GPDs.

Simulation studies proved that the EIC can perform accurate measurements of DVCS cross

sections and asymmetries in a very fine binning and with a very low statistical uncertainty [226]. This pioneering assessment of the capability of the EIC to constrain GPDs solely relies on global fits of DVCS measurements. Figure 7.39 shows the uncertainties of GPDs extracted from current data (blue bands) and how they are constrained after including the EIC pseudo-data into the fits (orange bands).

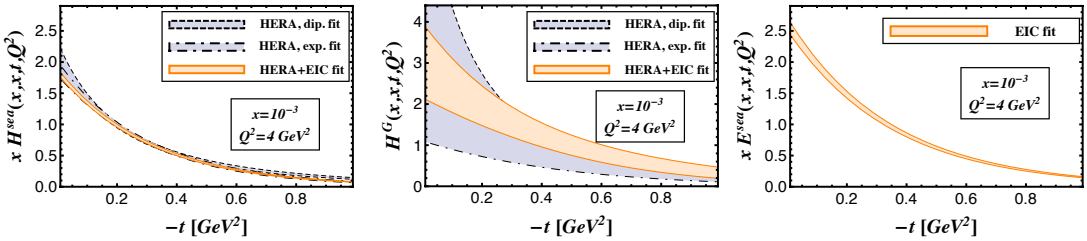

Figure 7.39: Extraction of GPD H for sea quarks (*left*) and gluons (*center*) and GPD E for sea quarks (*right*) at a particular x and Q^2. The violet band is the uncertainty obtained excluding the EIC pseudo-data from the global fit procedure [226].

This study demonstrated that the EIC can largely improve on our current knowledge of GPD H for gluons as shown in Fig. 7.39. Moreover, a precise measurement of the transversely polarized target spin asymmetry A_{UT}, which allows for a decomposition of GPD H and E contributions, leads to the accurate extraction of GPD E for the sea quarks, which at the moment remains almost unconstrained [226].

Diffractive events are known to constitute a large part of the cross section in high-energy scattering. In Refs. [227–229], access to GPDs is suggested in a diffractive process where a GPD driven subprocess ($\mathcal{P}N \to \gamma^*(Q'^2)N'$ or $\mathcal{P}N \to MN'$, where $\mathcal{P}$ is a hard Pomeron and M a meson) is triggered by a diffractive $\gamma^*(Q^2) \to \rho\mathcal{P}$ process as shown in Fig. 7.40. The kinematical domain is defined with a large rapidity gap separating the ρ from the γ^*N' or MN' final state and a small momentum transfer between the initial and final nucleons.

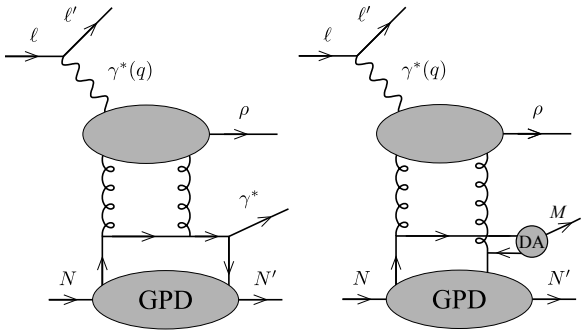

Figure 7.40: Leading order diagram for diffractive DVCS (left panel) and diffractive two-meson (right panel) production, with a large rapidity gap between the forward ρ and the remaining γ^*N' or MN' final state.

Contrary to the usual DVCS and TCS processes, the integration over the quark momentum fraction in the amplitudes is restricted to a smaller domain ($-\xi < x < \xi$), with gluons not entering due to C-parity conservation. The skewness parameter ξ is not related to x_B as

in DVCS, giving access to large ξ values even for large energy processes [227, 228]. In the meson production process, as in DVMP, the nature of the meson and its polarization select particular types of GPDs (vector, axial vector, transversity). The amplitudes are energy independent at leading order, and would acquire a mild energy dependence when large energy evolution is turned on. Cross section projections for the ρM-production process at EIC kinematics were studied in Ref. [229]. Detailed EIC simulations for both processes are in progress [230].

In [231–234], a new class of processes is proposed to access GPDs through $\gamma + N \to \gamma + M + N'$ and $\gamma + N \to \gamma + \gamma + N'$, focusing on the regime where $M^2_{\gamma M}$ or $M^2_{\gamma\gamma}$ provides a hard scale. The connection with GPDs relies on the fact that the fixed angle subprocess $\gamma(q\bar{q}) \to \gamma + M$ or $\gamma(q\bar{q}) \to \gamma + \gamma$ factorizes from GPDs.

In the photoproduction of $\gamma\gamma$, the hard sub-process gives access to GPDs at the special point $x = \pm\xi$ [232]. The photoproduction of a photon-meson pair, for example $\gamma\rho$ [231], is on the other hand sensitive to chiral-odd (transversity) GPDs. Charge conjugation constraints dictate that only chiral-odd GPDs contribute to the production of a transversely-polarised ρ, while chiral-even GPDs contribute to the meson's longitudinal polarisation. Separating out the polarisation states via measurements of the ρ decay products enables separation of the chiral-even and transverse GPDs. This process additionally benefits from a suppression of gluon GPDs in the amplitude, which typically introduce large NLO corrections. Simulations of the process at EIC kinematics are underway [235]. The chiral-even sector ($M = \pi$ or ρ_L) can yield a very large new set of observables, complementing measurements of DVCS, TCS and DVMP which involve the same GPDs. In addition, the case where $M = \pi^0$ provides a new way to access GPDs of gluons.

A novel method to extract GPDs has recently been proposed [236], which is based on comparison of ρ- and π-meson production cross sections in charged current processes. These processes are numerically suppressed compared to photoproduction and pose significant experimental challenges, yet are within the reach of the Electron Ion Collider, as described in Sect. 8.4.8.

Impact parameter distributions

Impact parameter distributions can be reconstructed by taking a Fourier transform of the GPDs in the variable t at $\xi = 0$. These distributions represent densities of partons with a given momentum fraction of x as a function of the position $\mathbf{b}_\perp$ from the center of momentum of the nucleon in the transverse plane [237]. A first attempt to obtain this information directly from photon electroproduction measurements was illustrated in Refs. [238, 239], using a model-dependent extrapolation to the point $\xi = 0$ that is not accessible experimentally. Recently, dispersion-relation techniques have been used in Ref. [240] to constrain the GPDs at $\xi = 0$ from data. Both these analyses confirm that the width of the impact-parameter distribution for unpolarized quarks in unpolarized protons has a very peaked transverse profile in the limit of $x \to 1$. This behaviour comes from the fact that, in this limit, the active quark is always very close to the transverse center of momentum [237,241].

It suggests that the higher-x valence quarks are localised closer to the centre of the nucleon than the lower-x sea quarks, which have a wider distribution in the transverse plane.

The DVCS-based EIC impact study of Ref. [226] showed how Fourier-transforming the GPDs constrained at the EIC, it is possible to extract the densities quarks and gluons in the impact parameter space, as shown in Fig. 7.41.

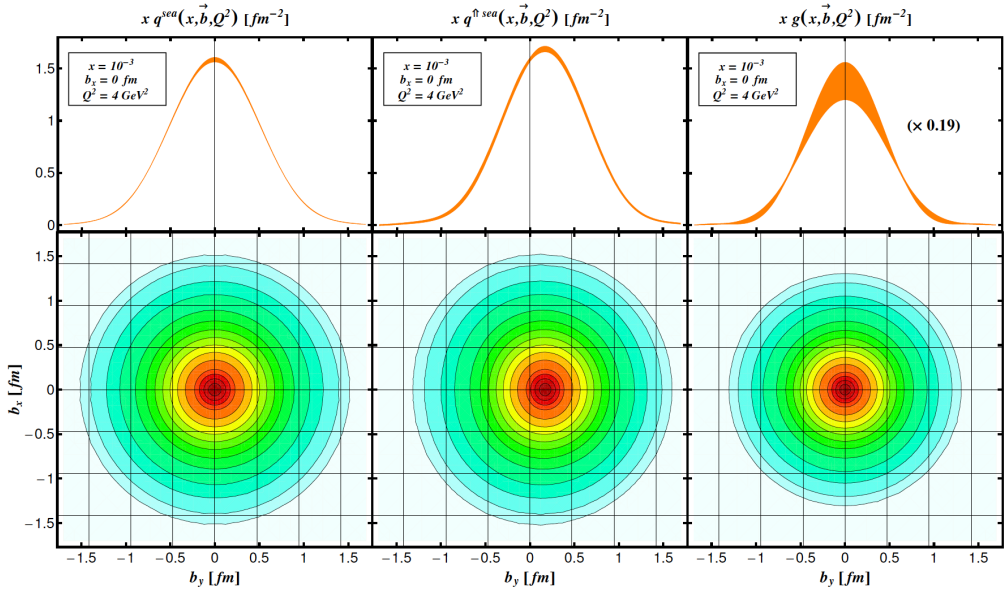

Figure 7.41: Parton densities at $x = 0.001$ and $Q^2 = 4$ GeV^2 versus impact parameter, obtained from a combined fit to the HERA collider and EIC pseudo data. Relative partonic densities (lower row) and their values at $b_x = 0$ for the unpolarized sea quark of an unpolarized proton (left), a transversely polarized proton (middle), and the unpolarized gluon of an unpolarized proton (right), its value is rescaled by a factor 0.19.

While this study is based only on measurements of DVCS, simulation studies have also proven how EIC can provide high precision measurements of the $|t|$-differential cross section of heavy vector mesons [225, 242]. More studies of measurements of light and heavy mesons, performed in the context of this yellow report, are discussed in Sec. 8.4.5. A Fourier-transform of the $|t|$-differential cross section for the production of heavy vector mesons can help to visualize the uncertainty achievable on the gluon distributions in the impact parameter space, though it still contains a contribution from the small but finite size of the meson, which needs to be disentangled in a full GPD analysis. Figure 7.42 shows the projected impact-parameter-dependent distributions of the gluon measurable at the EIC, enabling us to accurately probe the spatial distribution of gluons over two orders of magnitude in x, up to the region where the dominant partons are valence quarks.

Impact studies in Ref. [226] assume a measurement of the proton four-momentum transfer, $|t|$, in a very wide range, starting with the physical minimum $|t|_{min} \sim 0.03$ GeV^2 up to $|t| = 1.6$ GeV^2 which, in a Fourier transform, corresponds to large values of the impact parameter. Studies by the same authors show that limiting the measured $|t|$-range would

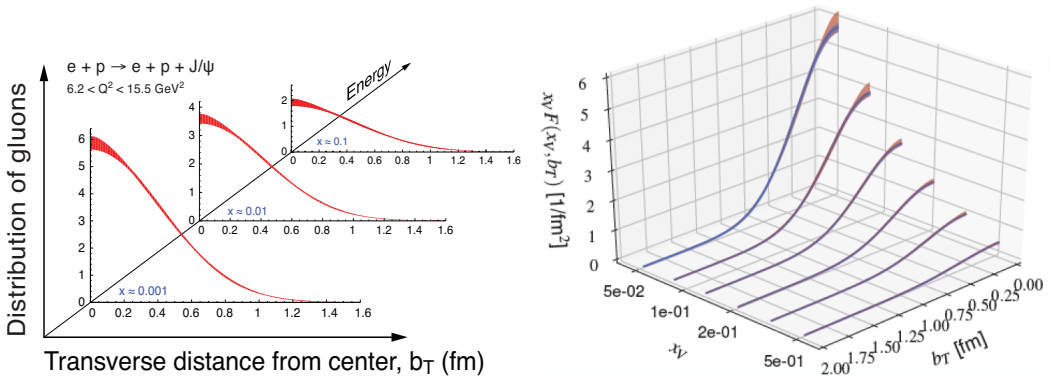

Figure 7.42: Projected EIC uncertainties on the measurement of the distribution of the gluon density versus the transverse distance from the center of the nucleon, resulting from differential cross section measurements of J/Ψ (left) and Υ (right). The gluon distributions uncertainty bands are plotted for a fixed Q^2 bin and three different values of x.

severely impact the precision of the extracted partonic densities, as shown in Fig. 7.43. The bands represent the uncertainty from different extrapolations to the regions of unmeasured (very low and very high) values of $|t|$.

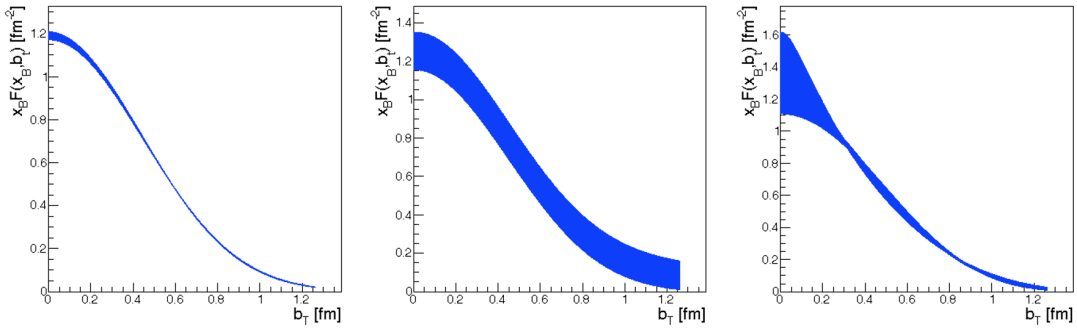

Figure 7.43: The combined average impact parameter dependent partonic density obtained from a Fourier transform of the DVCS cross section measured at the EIC assuming different $|t|$ acceptances. The bands represent the parametric errors in the fit and the uncertainty from different extrapolations to the regions of unmeasured (very low and very high) $|t|$ of the scattered protons. Left: $0.03 < |t|$ (GeV^2) < 1.6; Middle: $0.2 < |t|$ (GeV^2) < 1.6 GeV/c; Right: $0.03 < |t|$ (GeV^2) < 0.65.

Form factors of the energy-momentum tensor

GPDs also offer the unique and practical opportunity to access the energy-momentum tensor (EMT) form factors, which are canonically probed through gravity. There are four independent EMT form factors for the separate quark and gluon contributions, usually referred as $A(t)$, $J(t)$, $D(t)$ and $\bar{C}(t)$. The first three form factors can be related to x-moments of the GPDs, and at $t = 0$, the corresponding "charges" for quarks and gluons give, respec-

tively, the fraction of nucleon momentum carried by the partons, Ji's relation [53] for the quark and gluon contribution to the total angular momentum of the nucleon (see Sect. **??**), and the D-term, which is sometimes referred to as the "last unknown global property" of the nucleon [243]. Furthermore, the $\bar{C}(t)$ form factor is related to the EMT trace anomaly and plays a relevant role in the generation of the nucleon mass (see Sect. 7.1.4). The information encoded in the EMT form factors is revealed in the so-called Breit frame [243, 244] and has been discussed recently in other frames in Refs. [105, 245]. Working in the Breit frame, the D-term form factor can be related to the spatial distribution of shear forces $s(r)$ and pressure $p(r)$. The relation for the shear forces holds also for quarks and gluons separately, while it is defined only for the total system in the case of pressure. In this way, the form factor $D(t)$ provides the key to mechanical properties of the nucleon and reflects the internal dynamics of the system through the distribution of forces. Requiring mechanical stability of the system, the corresponding force must be directed outwards so that one expects the local criterion $2s(r) + p(r) > 0$, to hold, which implies that the D-term for any stable system must be negative, $D < 0$, as confirmed for the nucleon in models [246–248], calculations from dispersion relations [249] and lattice QCD [250, 251]. Another consequence of the EMT conservation is the condition $\int_0^\infty p(r) r^2 \mathrm{d}r = 0$, which shows how the internal forces balance inside a composite particle. This relation implies that the pressure must have at least one node. All models studied up to now show that the pressure is positive in the inner region and negative in the outer region, with the positive sign meaning repulsion towards the outside and the negative sign meaning attraction directed towards the centre. Recently, an analysis of the published JLab data measured at 6 GeV [252, 253] has provided the first experimental information on the quark contribution to the D-term form factor [254]. The D-term parameters fitted to the JLab data, with the assumption of a negligible gluon contribution, were used to obtain the radial pressure distribution. Within the uncertainties of the analysis, the distribution satisfies the stability condition, with a zero crossing near $r = 0.6$ fm. This analysis has been repeated in Ref. [255] using more flexible parametrization by neural networks to improve the analysis of the uncertainties. The obtained results show that presently available beam-spin asymmetry and cross-section measurements alone do not allow to draw reliable conclusions. The method itself, however, appears valid and may provide a conclusive extraction of the quark distribution in the future, when used in combination with other observables, more sensitive to the real part of Compton form factors and to the D-term (such as the DVCS beam-charge asymmetry or the production of lepton pairs), and with forthcoming data from present facilities (Jefferson Laboratory, COMPASS at CERN) and the EIC. Similarly, exploratory studies for the extraction of the other EMT form factors at the EIC are in progress. Measuring beam-charge asymmetries, the most sensitive probe to the D-term, requires a positron beam, which can be unpolarized. While this is not envisioned in the EIC baseline, there are no technical obstacles to this upgrade in the future.

Transition distribution amplitudes

New information can be accessed by studying the u-crossed channel of hard exclusive meson production. In the kinematics of $t \sim t_{\mathrm{max}}$ and $u \sim u_{\mathrm{min}}$, this process is characterized

by a non-zero baryon number exchange in the cross channel and can be studied in terms of non-perturbative objects known as Nucleon-to-meson Transition Distribution Amplitudes (TDAs) [256–259]. TDAs describe the underlying physics mechanism of how the target proton makes a transition into a π meson in the final state. One fundamental difference between GPDs and TDAs is that the TDAs require three parton exchanges between the TDA and the hard part. At leading-twist, there are 8 independent TDAs that can be classiffied in terms of the light-cone helicity of the exchanged quarks [260]. This opens the way to specific and detailed analysis of the helicity content of correlated quarks in the nucleon. Similarly to GPDs, after the Fourier transform in the transverse plane, TDAs also carry valuable information on the transverse location of hadron constituents and allow one in particular to quantify the effect of diquark clustering in nucleons [261]. In order to advance in the exploration and development of the TDA physics, the EIC, along with the measurements planned at other existing facilities, can play a crucial role (see Sect. 8.4.7 for kinematic studies).

7.2.3 Imaging of quarks and gluons in momentum space

Transverse momentum dependent distribution and fragmentation functions (TMDs) describe not only the partons' longitudinal momentum given by the variables x and z for distribution and fragmentation functions, respectively, but also the transverse momentum. Initially suggested as potential mechanisms for creating the unexpectedly large single transverse spin asymmetries in hadronic collisions [262, 263], they are now a staple for describing the three-dimensional spin and momentum structure of the nucleon and provide access to quantities that could previously not be studied. At an electron-ion collider the main access to TMDs comes over semi-inclusive DIS where in addition to the general DIS quantities x, Q^2, and y, one also identifies final state hadrons with a fractional energy z and transverse momentum p_T relative to the virtual photon direction. In several cases also azimuthal angles of incoming hadron spin and fragmenting hadron momentum relative to the lepton scattering axis are measured. Accounting for the transverse momentum degrees of freedom allows the extraction of non-perturbative TMDs and, ultimately, reconstructs the three-dimensional picture of hadrons in momentum space. The general description of semi-inclusive DIS can be found in [140, 264] and later additions for single hadron observables. Additional details of the momentum space image, such as flavor substructure, distribution of gluon transverse motion, and others, can be received from different other semi-inclusive processes, primarily di-hadron production and jet-based measurements.

The main theoretical tool for probing TMDs is the TMD factorization theorem and its extensions. Within the TMD factorization theorem one defines universal TMD distributions [265, 266] that are non-perturbative functions of two variables $x(z)$ and k_T, which parametrize longitudinal and transverse components of the parton's momentum. The theoretical framework of TMD factorization has been intensively developed during the last decades, and it has led to discoveries of new applicable domains and deeper connections with fundamental properties of QCD. Within the TMD factorization, structure functions